This is a postprint version of the following published document:

Thermal conductivity and diffusivity of Cu-Y alloys produced by different powder metallurgy routes

G. Carro[a], A. Muñoz[a], M.A. Monge[a], B. Savoini[a], A. Galatanu[b,] M. Galatanu[b], R. Pareja[a]

[a]*Universidad Carlos III de Madrid, Physic Department. Leganés- Madrid (Spain).*
[b] *National Institute of Materials Physics, Magurele-Bucharest (Romania).*

Full density Cu-1%Y and Cu-0.8%Y alloys have been produced by different powder metallurgy routes and subsequent hot isostatic pressing. Some of the alloys have been subjected to equal channel angular pressing (ECAP) via B_C route up to 8 passes. ECAP deformation homogenizes and refines the microstructure up to attaining a sub-micron grain structure. Thermal properties have been characterized by the laser flash method in the temperature range 373-773 K. The ECAP process, irrespective of the production route, enhanced the thermal conductivity to values similar to those for CuCrZr (ITER grade). The linear thermal expansion coefficient was temperature independent for all materials.

Keywords: Copper, Yttrium, Thermal Conductivity, ECAP, MA, Coefficient Thermal Expansion.

1. Introduction

The design of future fusion reactors implies to produce new materials with appropriate properties for working under extreme conditions. In particular, the components of the ITER cooling system must work in the temperature range 373-673 K, maintaining a high thermal conductivity and adequate mechanical properties. In addition, these materials have to exhibit a good resistance to the swelling effect produced by the interactions with high energy neutrons.

CuCrZr alloy, with composition Cu-(0.5-1.2%)Cr-(0.03-0.3%)Zr (wt%) is the reference candidate for heat sink materials in ITER [1]. Although it presents a good weldability and high fracture toughness at high temperature, under neutron irradiation it undergoes a loss of ductility at low temperature and a worsening of the strength at elevated temperatures, what limits its working temperature [2,3]. Besides, above 723 K the dissolution of the precipitates is activated and the degradation of the mechanical properties occurs.

The development of new oxide dispersion strengthened (ODS) Cu based materials to improve the mechanical properties of pure copper presents several advantages [4,5]. Firstly, the oxide dispersed particles, like Y_2O_3, are very stable with temperature and do not decomposed or dissolved in the temperature operative window of the Cu based materials.. Secondly, the presence of a fine dispersion of particles retards the recrystallization phenomenon, increases the resistance to softening at high temperatures and does not imply an appreciable decrease in the thermal conductivity. Previous studies have reported that in ODS Cu-Y_2O_3, the dispersion of Y_2O_3 nanoparticles gives place to an increase in the mechanical resistance of copper [6,7]. Furthermore, Neklyudov *et al.* have reported that the presence of a small amount of yttrium dispersed in copper reduces the damage of defects due to neutron irradiation [8].

In this work the thermal properties of Cu-Y alloys produced following different powder metallurgy routes, which include sintering by hot isostatic pressing (HIP), are presented. To assess the effect of the microstructure some specimens were subjected to an equal channel angular pressing (ECAP) thermo-mechanical treatment. The thermal properties were evaluated in the temperature range 373-773 K.

2. Experimental Procedure

2.1. Materials production and characterization

For the production of ODS Cu-1%Y (wt%), copper and yttrium powders with a purity of 99.9 % were used. The size of the powder particle was below 400 μm for yttrium and below 105 μm for copper. Firstly, the powders were blended in a turbular mixer for 4 hours under an argon atmosphere and later, milled in a high-energy planetary ball mill during 22 hours at 100 rpm under an argon atmosphere. The milling media were Cr-steel balls, being the ball/powder ratio of 7:1. The cold welding phenomenon was avoided on alternating short milling periods of 120 seconds with rest periods of 180 seconds. The milled powder was consolidated by HIP. The alloys were labeled as Cu-1YM.

For the ODS Cu-0.8%Y (wt%) fabrication, powder with nominal composition Cu-0.8wt%Y and particle size < 120 μm was produced by vacuum induction melting and subsequent atomization in high purity Ar gas. The purity of the raw Cu and Y powders was 99.9% and 99%, respectively. The atomized powder was consolidated by HIP and the obtained alloy labeled as Cu-0.8Y. To homogenize and refine the initial microstructure of the atomized powder, it was milled in a high energy planetary ball mill during 40 hours at 100 rpm under an Ar atmosphere. The resulted alloy obtained after HIP consolidation was labeled as Cu-0.8YM. The milling media were Cr-steel balls with a

ball/powder ratio of 5:1. The goal was to analyze the effect of the milling process in the morphology and size of the Y particles and check if the milling process promotes the formation of Y_2O_3 particles. In all cases the HIP treatments were performed for 2 h at 1123 K and 179 MPa. Previously, the powders had been encapsulated into a steel can that was tight sealed after degassing at 573 K for 24 h in vacuum. A cylindrical rod Ø 8 mm × 120 mm was produced for each alloy.
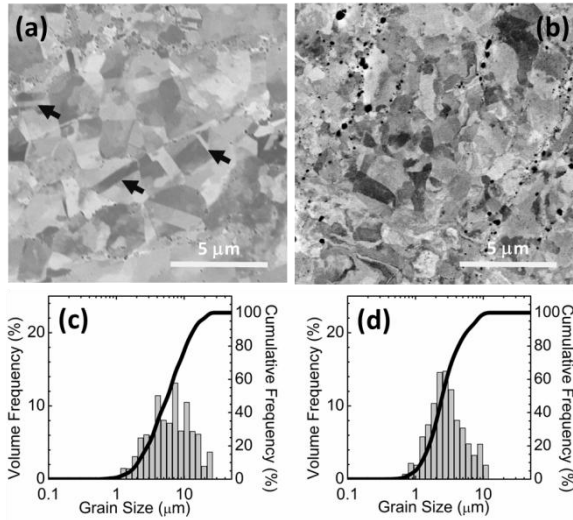

Fig. 1. SEM images from: (a) Cu-1YM and (b) Cu-1YME. Grain size distributions (obtained from optical microscopy images) of: (c) Cu-1YM and (d) Cu-1YME. Black arrows point to twins.

Cu-1YM, Cu-0.8Y and Cu-0.8YM specimens were submitted to an ECAP treatment at 623 K following the B_C route. The ECAPed samples were denoted as Cu-1YME, Cu-0.8YE and Cu-0.8YME. The sample Cu-0.8YE was submitted to 8 passes, whereas samples Cu-1YME and Cu-0.8YME were submitted to only 4 passes. Density measurements were carried out by a He ultrapycnometer. The oxygen content was determined with a time-of-fight mass spectrometer LECO. The microstructure was analysed from the images obtained with an ultra-high resolution scanning electron microscope TENEO (FEI). The Vickers microhardness tests were carried out by applying a charge of 9.81 N.

2.2. Thermal measurements

Thermal diffusivity and specific heat were measured using the Laser Flash method with a LFA 457 apparatus (Laser Flash Analyses) [9]. The sample sizes were 9.9 ×9.9×3 mm³. The measurements were performed from room temperature to 773 K with a heating rate of 5 K/minute. Three measures were done for each condition, being the uncertainty ~2 %. The thermal conductivity, λ, was calculated from the expression: $\lambda = \alpha \cdot C \cdot \rho$. α is the thermal diffusivity, C is the specific heat at constant pressure and ρ is the density. The linear thermal expansion was measured with a dilatometer DIL 402 on samples whose sizes were 3×3×10 mm³.

Corresponding author: gcarro@fis.uc3m.es

The measurements were done in vacuum from room temperature to 773 K, with a heating rate of 5 K/minute.

3. Results and discussion

The results of the density and Vickers micro-hardness measurements are shown in Table 1. The densification was determined after calculating the theoretical density using the phase rule. As the values are above 99% it is considered that a full densification was achieved for all materials. It is noted that materials subjected to ECAP treatments exhibit a higher microhardness. The ECAP process gives place to a reduction of the grain size that induces an increase in the material strength. The oxygen contents of the alloys are presented in Table 2. The alloys that were produced from milled powder exhibit higher oxygen content. It means that an appreciable amount of oxygen is incorporated to the alloy during the milling step. As yttrium has a greater affinity for oxygen than copper, the formation of Y_2O_3 reinforcing particles is expected.

Table 1. Characteristic parameters of the consolidated materials. The fabrication routes have been specified (at: atomization, mill: milling).

Material		ρ_{exp} (g/cm³)	ρ_{exp}/ρ_{th} (%)	H_V (GPa)
Cu-0.8Y	at+HIP	8.859	99.7	0.66 ± 0.02
Cu-0.8YE	at+HIP+ECAP	8.853	99.6	1.23 ± 0.02
Cu-0.8YM	at+mill+HIP	8.822	99.3	0.98 ± 0.01
Cu-0.8YME	at+mill+HIP+ECAP	8.821	99.2	1.24 ± 0.03
Cu-1YM	mill+HIP	8.782	99.0	0.90 ± 0.07
Cu-1YME	mill+HIP+ECAP	8.780	99.0	1.20 ± 0.04

Table 2. Oxygen content of the consolidated materials and linear thermal expansion coefficient (LCTE). The LCTE of CuCrZr and pure Cu were measured at 623 K [12].

	Oxygen (%wt)	LCTE (10^{-6} K⁻¹)
Cu-0.8Y	0.0061 ± 0.003	18.6 ± 0.01
Cu-0.8YE	0.0054 ± 0.003	18.4 ± 0.01
Cu-0.8YM	0.154 ± 0.003	17.7 ± 0.02
Cu-0.8YME	0.160 ± 0.003	19.2 ± 0.06
Cu-1YM	0.121 ± 0.003	18.1 ± 0.07
CuCrZr-IG	--	18.0
Pure Cu	--	16.6

The microstructure of the alloys is shown in Figs 1 and 2. After HIP, Cu-1YM and Cu-0.8YM exhibit a great number of twins (Figs 1(a) and 2(c)). These alloys were sintered from powder subjected to a milling process, which introduces a large amount of deformation producing a wide variety of defects like deformation stacking faults. During sintering at high temperature, the recrystallization process deals to the formation of annealing twins [10]. In contrast, the presence of twins is no observed in the Cu-0.8Y (Fig. 2(a)), which has been obtained from atomized powders with a well-recrystallized microstructure [7]. In all cases it is observed the formation of Y-rich particles (black contrast) that are distributed inside the matrix grains and at the grain boundaries.
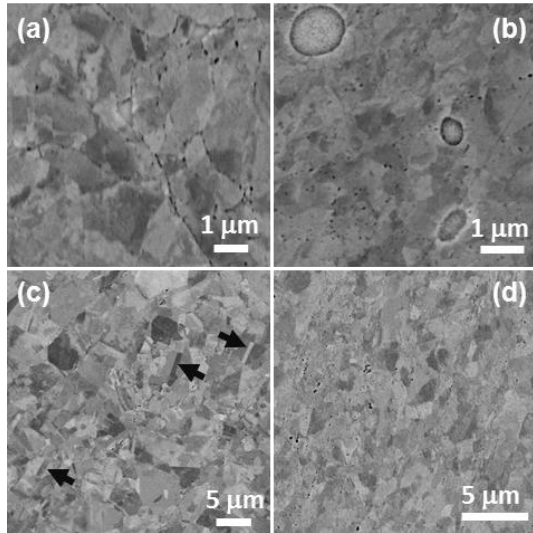
Fig. 2. SEM images from: (a) Cu-0.8Y, (b) Cu-0.8YE, (c) Cu-0.8YM and (d) Cu-0.8YME. Black arrows point to twins.
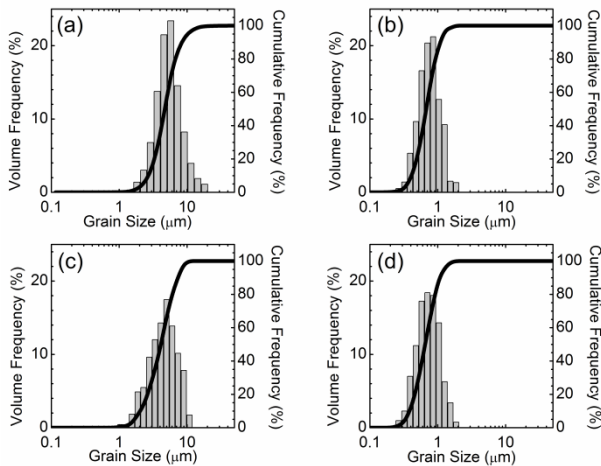

Fig. 3. Grain size distribution. (a) Cu-0.8Y, (b) Cu-0.8YE, (c) Cu-0.8YM and (d) Cu-0.8YME.

The ECAP process gives place to a reduction of the grain size and a microstructure with grains more equiaxed, as observed in Figs. 1 and 2. Although in these pictures the presence of twins is difficult to appreciate, the ECAP process has introduced a great deformation in the alloy. In addition to the grain refinement, a significant homogenization of the grain size is achieved, as it can be appreciated in the reduction of the width of the grain size distributions depicted in Figs. 1 and 3. For Cu-1YM the mean grain size decreases from 6.1 μm to 2.5 μm, for Cu-0.8Y from 4.8 μm to 0.67 μm and for Cu-0.8YM from 4.3 μm to 0.66 μm. It is important to note that these mean grain size values are estimated from the volume frequency histograms of the grain size distributions that give larger values than those obtained from the grain frequency histograms.

Thermal diffusivity is a material-specific property for characterizing the rate of transfer of heat inside the material. It allows assessing the time constant of the heat diffusion process. The thermal diffusivity of the different alloys in the temperature range 373-773 K is displayed in Fig. 4(a). For all materials a nearly constant value was obtained for the whole temperature range and no significant differences among alloys were found. The ECAP process did not shown any effect on it.

Fig. 4(b) shows the specific heat of the alloys versus temperature. This parameter quantifies the ability of a material for storing thermal energy. For a pure metal, both the free electrons and the phonons contribute to the specific heat, although at low temperature the electronic contribution dominates. For a metallic alloy, at temperatures above the Debye temperature, which is ~343 K for pure copper [11], the lattice contribution predominates. In our case T>300 K, so the measured specific heat is primarily due to the lattice contribution. The uncertainty was ~3 %. From Fig.4(b) it is inferred that the ECAP process raises the specific heat of the alloys to a similar value regardless of the production route.

The thermal conductivity has been calculated from thermal diffusivity and specific heat values. The resulting values are plotted in Fig. 4(c). The higher thermal conductivity values were found for the ECAPed alloys, i.e. Cu-0.8YME and Cu-0.8YE, with values close to that of CuCrZr, ~350 Wm^{-1}K^{-1} [12].

The effects of the ECAP were found to be the homogenization of the microstructure and the overall decrease of the grain size. Although it implies an increase of the number of grain boundaries and therefore of the number of barriers for the phonon propagation, it seems that it is advantageous for the thermal conductivity. After a certain number of passes, the ECAP process can eliminate the texture present in the sample and also improves the bonding between the grain boundaries, what should enhance the heat conduction.

The evolution of the linear thermal expansion with the temperature is also a relevant feature for a cooling system component. Fig. 4(d) shows the dependence of $\Delta L/L_o$ in the temperature range 300-575 K. A linear dependence is observed, which implies a constant linear thermal expansion coefficient, CTE. The CTE values obtained from the fitting of the curves are presented in Table 2. It is noted that these values are very similar and very close to that of CuCrZr.

4. Conclusions

Fully density Cu-1%Y and Cu-0.8%Y alloys have been produced via powder metallurgy routes that include sintering by HIP and, in some cases, a previous milling. Some of the alloys were subjected to an ECAP process following a B$_C$ route. In case the initial powders

Corresponding author: gcarro@fis.uc3m.es

were milled, it was observed the presence of twins. The ECAP process deals to a homogenization of the microstructure and a decrease of the grain size.
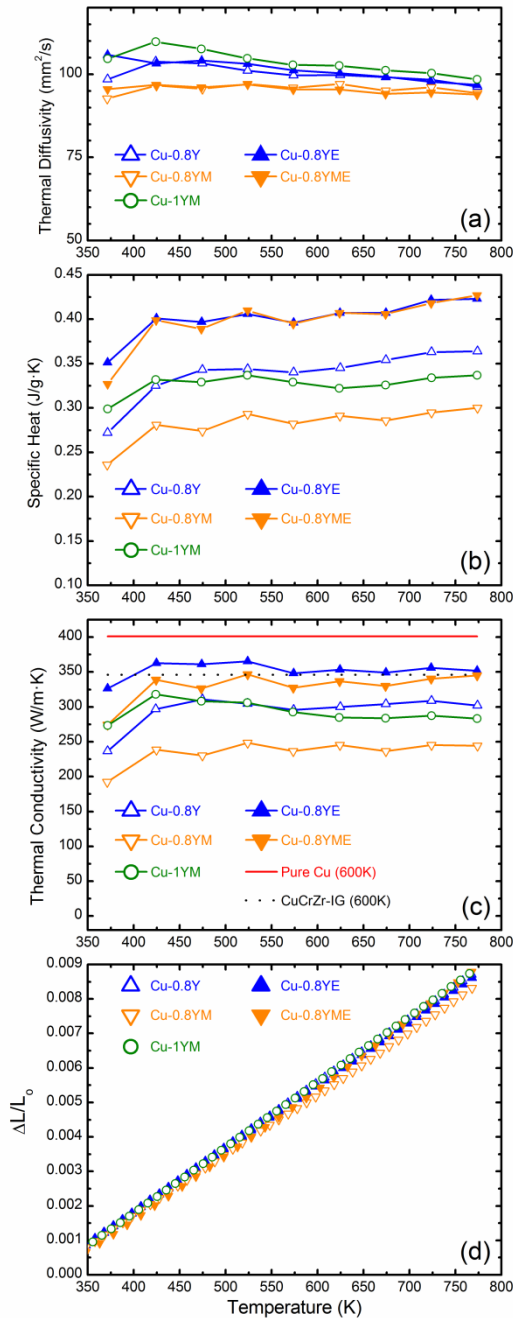

Fig. 4. (a) Thermal diffusivity of the alloys measured by the laser flash method. (b) Specific heat and (c) Thermal conductivity of the different alloys. The thermal conductivity of pure Cu and CuCrZr (ITER grade) at 600 K is also represented. (d) $\Delta L/L_o$ versus T for the different alloys.

The thermal measurements have shown that the ECAP process improves the thermal conductivity of all the alloys, getting values very close to that of CuCrZr (ITER grade). The linear thermal expansion is very similar for all the alloys and it remains constant in the temperature range 300-575 K. Additional fracture toughness measurements would be desirable in order to compare them with those of CuCrZr.

6. References

[1] Fabio Crescenzi, C. Bachmann, M. Richou, S. Roccella, E. Visca, J.-H. You, Design study of ITER-like divertor target for DEMO, Fusion Engineering and Design, Volumes 98–99, October 2015, Pages 1263–1266.

[2] M. Li, S.J.Zinkle, Comprehensive Nuclear Materials Vol. 4 (2012) 667-690, Editor Rudy J.M. Konings, Published by Elsevier Ltd.

[3] A.D. Ivanov, A.K. Nikolaev, G.M. Kalinin, M.E. Rodin, Effect of heat treatments on the properties of CuCrZr, Journal of Nuclear Materials 307-311 (2002) 673-676.

[4] Viseslava Rajkovic, Dusan Bozic, Aleksandar Devecerski, Milan T. Jovanovic, Characteristic of copper matrix simultaneously reinforced with nano- and micro-sized Al_2O_3, Materials Characterization 67 (2012) 129-137.

[5] Meslet Al-Hajri, Aldo Melendez, R. Woods, T.S. Srivatson, Influence of heat treatment on tensile response of an oxide dispersion strengthened copper, Journal of Alloys and Compounds 290 (1999) 290-297.

[6] G. Carro, A. Muñoz, M.A. Monge, B. Savoini, R. Pareja, C. Ballesteros, P. Adeva, Fabrication and characterization of Y_2O_3 dispersion strengthened copper alloys, J. Nucl. Mater. 455 (2014) 655-659.

[7] G. Carro, A. Muñoz, M.A. Monge, B. Savoini, R. Pareja Microstructural and mechanical characterization of Cu-0.8 wt.%Y, Fusion Engineering and Design, Volumes 98–99 (2015) 1941–1944 .

[8] I.M. Neklyudov, V.N. Voyevodin, S.V. Shevtchenko, V.F. Rybalko, N.V. Kamychantchenko and I.A. Belenko Changes of structure and properties of yttrium doped copper at deformation, annealing and irradiation, Journal of Nuclear Materials 258-263 (1998) 1040-1044.

[9] S. Min , J. Blumm, A. Lindemann A new laser flash system for measurement of the thermophysical properties Thermochimica Acta 455 Issues 1–2 (2007) 46–50.

[10] W.Z. Han, S.D. Wu, S.X. Li and Z.F. Zhang, Origin of deformation twinning from grain boundary in copper, Applied Physics Letters 92 (2008) 221909.

[11] Kittel Charles, Introduction to Solid State Physics, John Wiley&Sons, 2004.

[12] G. Purcek, H. Yanar, M. Demirtasb, Y. Alemdag, D.V. Shanginac, S.V. Dobatkin, Optimization of strength, ductility and electrical conductivity of Cu–Cr–Zr alloy by combining multi-route ECAP and aging 649 (2016) 114–122.
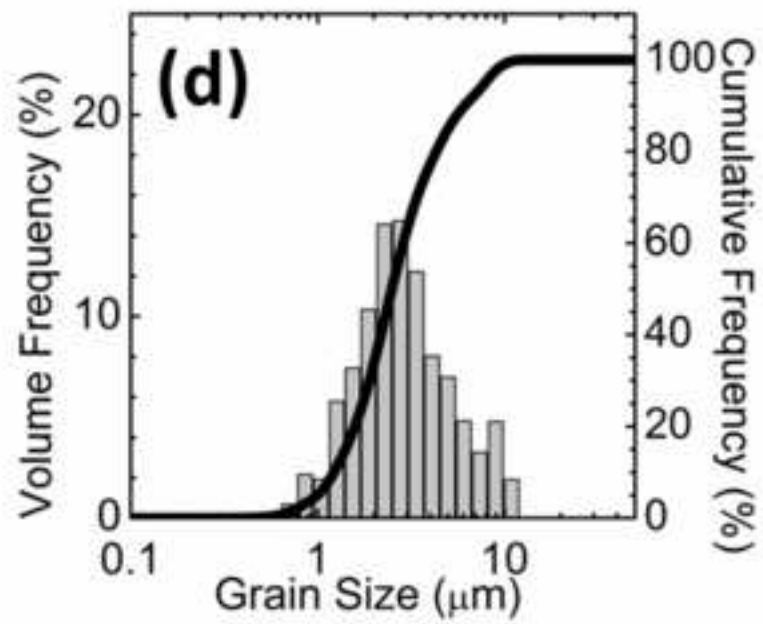
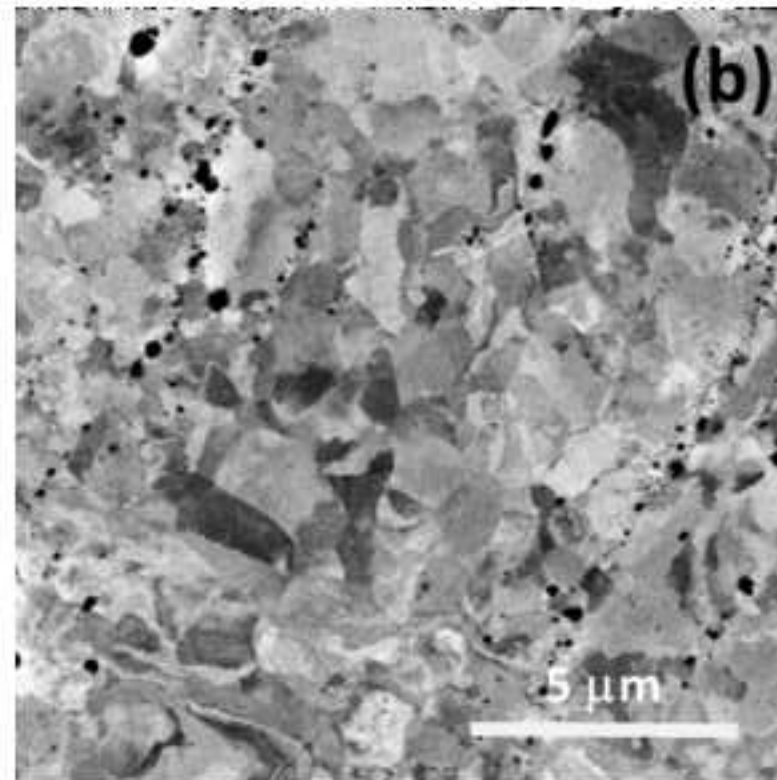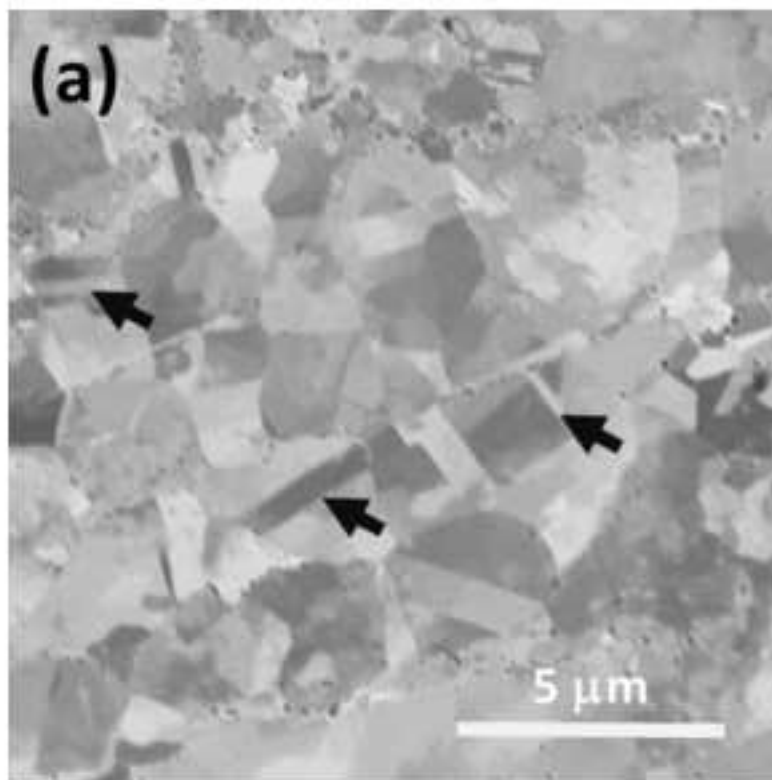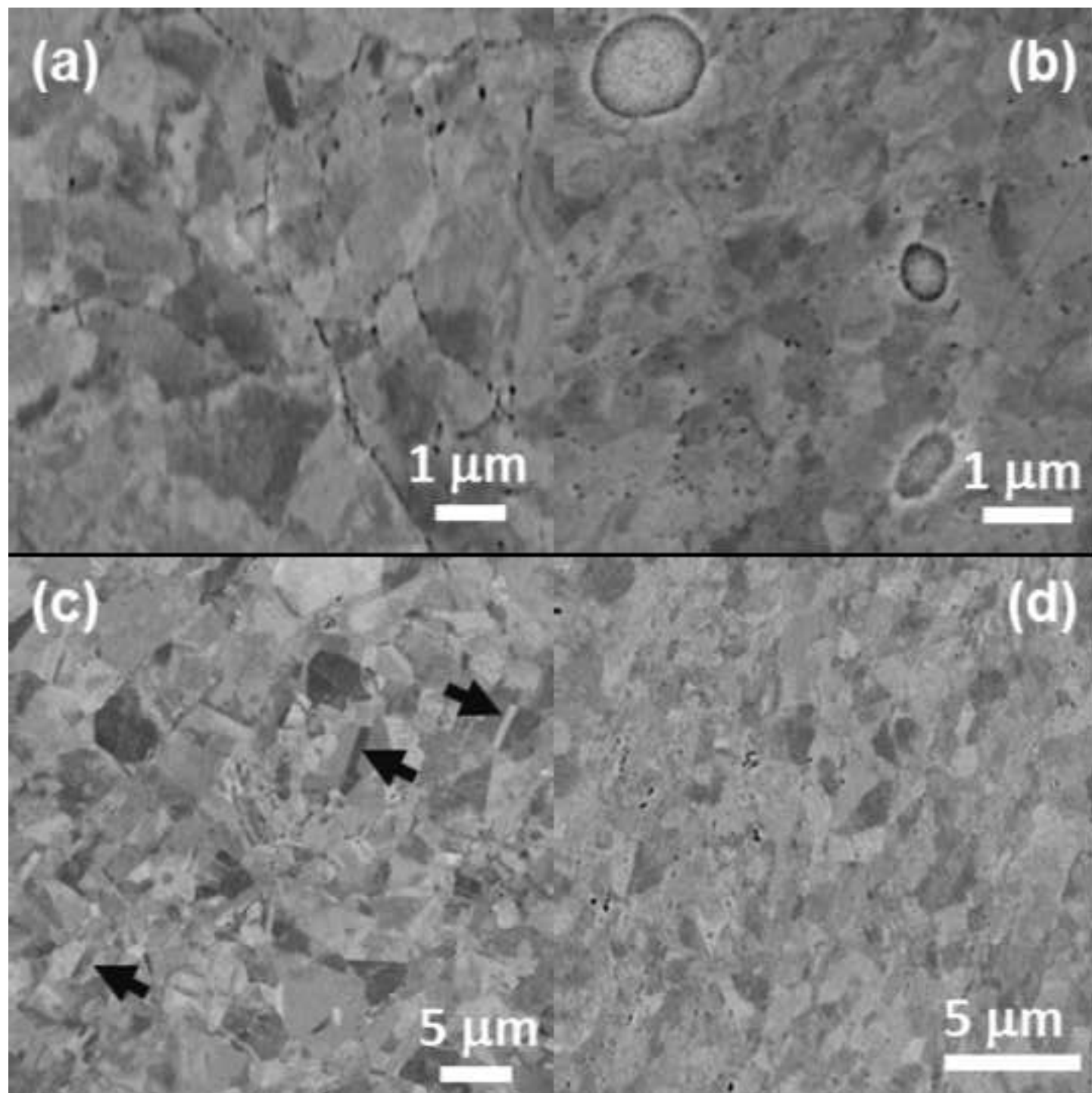Corresponding author: gcarro@fis.uc3m.es
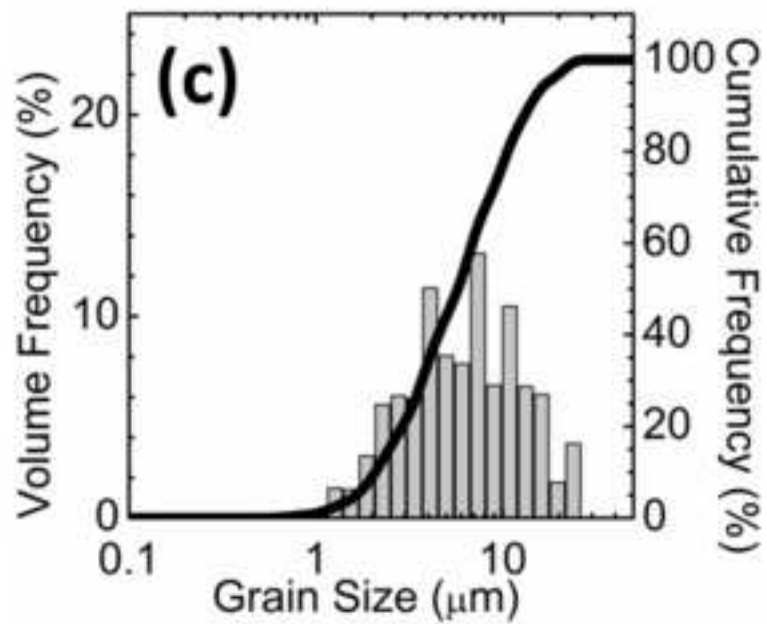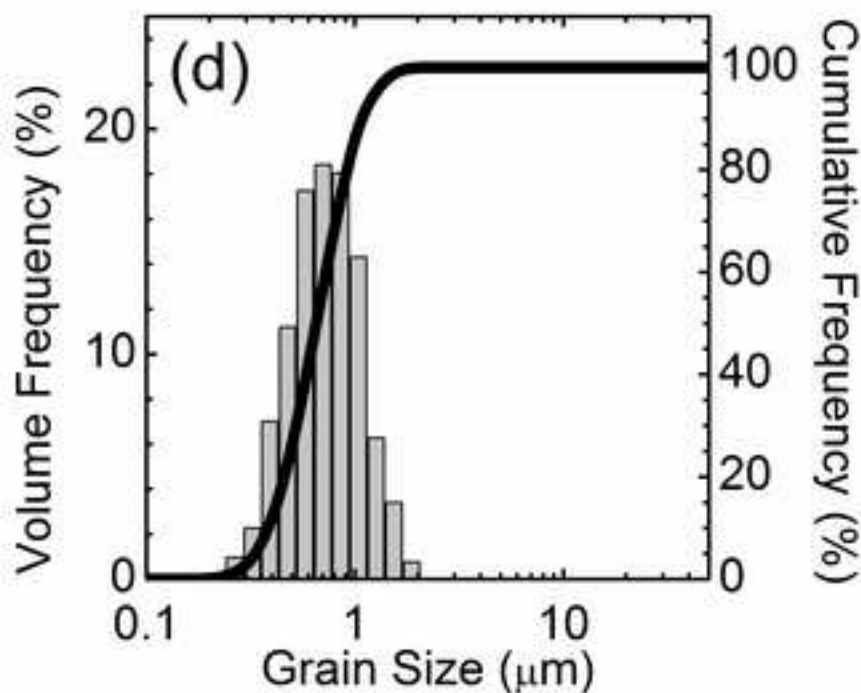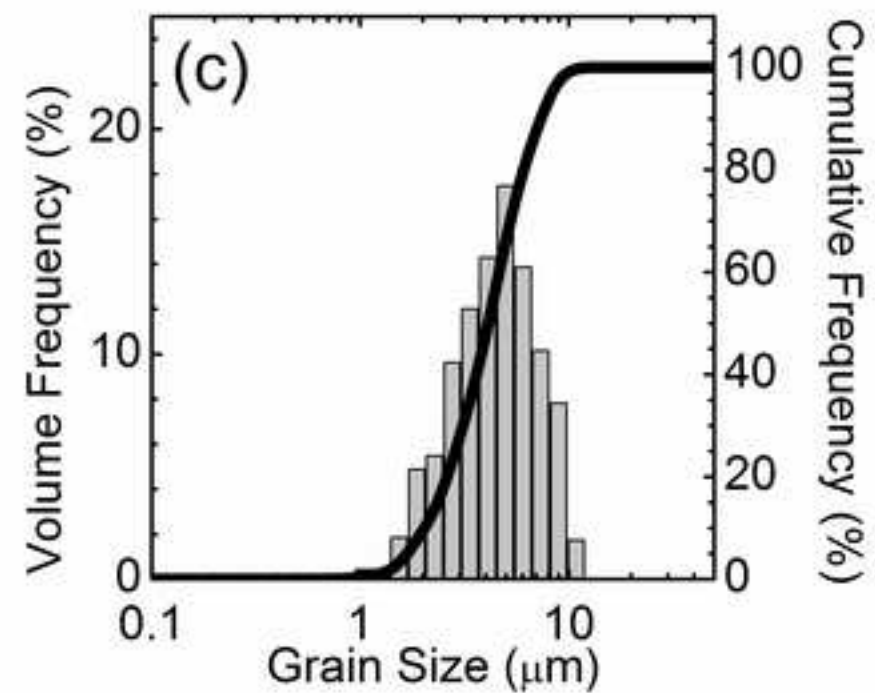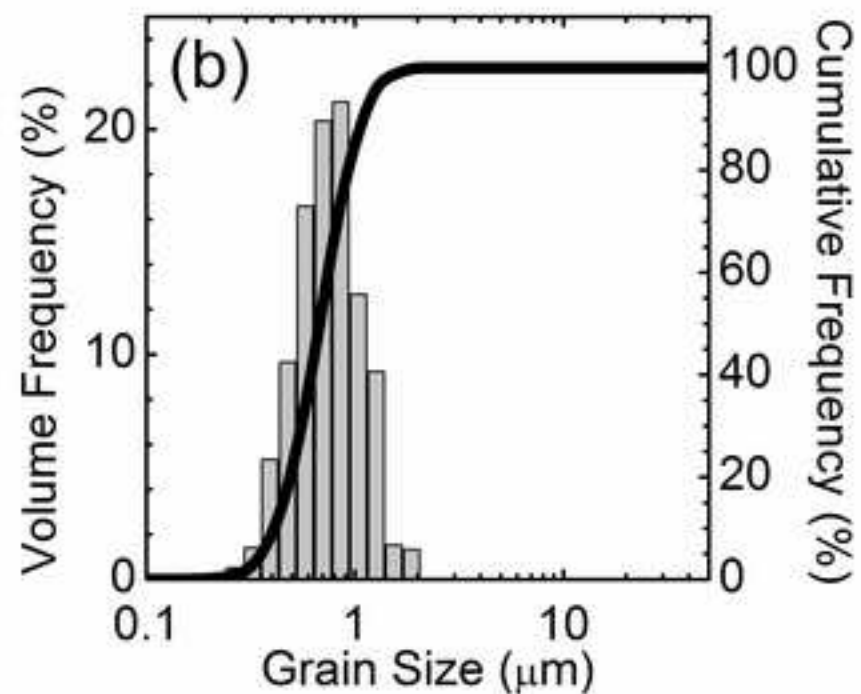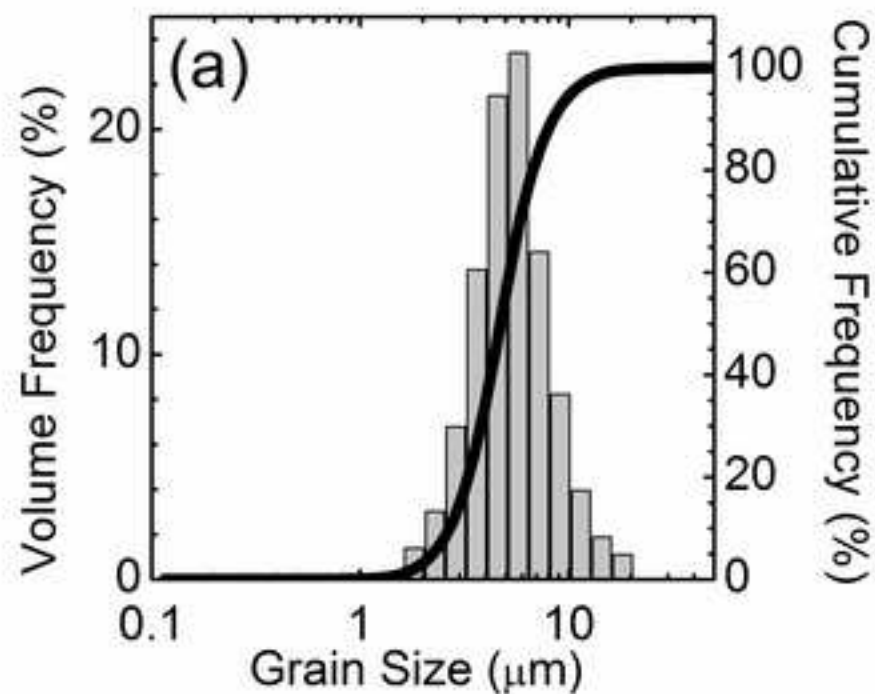
Figure2
Click here to download high resolution image

Figure4
Click here to download high resolution image